Achieving High-Resolution Electrohydrodynamic
Printing of Nanowires on Elastomeric Substrates
through Surface Modification

Ping Ren¹, Yuxuan Liu², Runqiao Song², Brendan O'Connor², Jingyan Dong¹,* and Yong Zhu²,*

KEYWORDS: EHD printing, stretchable electronics, silver nanowires, PDMS surface modification, UVO treatment, polydopamine coating.

Abstract

Stretchable electronics based on nanomaterials has received much interests recently. However, it is challenging to print 1-D nanomaterials (e.g., nanowires) with high resolution on stretchable elastomeric substrates. Electrohydrodynamic (EHD) printing has been used to print 1D nanomaterials such as silver nanowires (AgNWs) on stretchable substrates, but the resolution and electric conductivity of the printed patterns are typically low due to the poor wettability of the ink on the surface of the substrates. This paper reports a systematic study of two surface modification methods, UV-ozone treatment and dopamine coating, to modify the surface of polydimethylsiloxane (PDMS), which enables reliable and tunable EHD printing of AgNWs. The dynamic contact angle and the contact angle hysteresis were systematically studied to understand and evaluate the two surface modification methods. This work further investigates the hydrophobic stability of the two surface modification methods that is of critical relevance to the EHD printing as it determines the shelf life of the treated samples. The effects of treatment dose and aging on the EHD printing performances, such as resolution and conductivity, were studied to find the feasible ranges of the parameters for the surface treatment and printing process. The surface modification methods along with the proper printing conditions can be selected to tailor and optimize the printing performance. A wearable electronic patch with a fractal pattern of AgNWs is printed on the modified PDMS substrate to demonstrate the potential of the reported surface modification for reliable EHD printing of AgNWs for stretchable devices.

1. Introduction

Stretchable electronics is attracting significant attention as it enables a myriad of promising applications where electronic devices can undergo large deformation and/or form intimate contact with curvilinear surfaces. 1-7 There are two main approaches for fabricating stretchable electronic devices. One is the top-down microfabrication of inorganic materials, which has led to a variety of exciting stretchable devices such as epidermal electronics ^{8, 9} and conformal bio-integrated electronics. The process typically involves photolithography, vacuum-based deposition techniques and etching, which can be complicated and relatively expensive. The other approach is based on the assembly of bottom-up synthesized nanomaterials. A plethora of nanomaterials have been explored for fabricating stretchable electronic devices showing excellent performances. 14-20 However, a major challenge for this approach lies in facile, scalable and low-cost nanomanufacturing.

Printed electronics refers to a type of electronics that are created by a variety of printing technologies. As a bottom-up manufacturing method, the key advantages of printing include low-cost manufacturing with high throughput, ability to fabricate functional nanomaterials such as nanoparticles and nanowires, compatibility with a wide range of substrates including stretchable ones, and relative ease for heterogeneous integration.²¹ Conventional printing techniques such as stencil printing, gravure printing, screen printing and inkjet printing traditionally use metal nanoparticles as the conducting materials for inks. Recently, one-dimensional (1-D) nanomaterials that include metal nanowires are emerging as a new generation of conducting materials for printing due to the excellent electrical conductivity and high stretchability as a result of the random percolation network.²²⁻²⁵ However, it remains a challenge to print 1-D nanomaterials with high resolution while retaining high conductivity, especially on stretchable elastomeric substrates.

Electrohydrodynamic (EHD) printing, 26,27 as a non-contact printing technique, has been reported to print high-resolution (i.e., submicron) patterns. Typical EHD printing system uses electric fields rather than thermal or acoustic actuation to produce the ink flow. $^{26-33}$ The applied electric field deforms the meniscus at the printing nozzle to form a cone shape (i.e. Taylor cone), making it possible to print features much smaller than the nozzle size. As a result, a larger nozzle can be used to avoid nozzle clogging, while still capable of producing high-resolution features. Considering that the length of metal nanowires is typically >10 μ m, conventional inkjet printing is difficult to print high-resolution features. EHD printing, however, can reliably print high-resolution features using a larger nozzle without the issue of nozzle clogging.

Nowadays, electrohydrodynamic printing has become a promising approach for the fabrication of the nanowire-based devices, as it is capable of printing ultra-fine nanowires in high-precision patterns. ³⁴⁻³⁸ Our recent work³⁴ demonstrated the feasibility of printing AgNWs with high resolution and high conductivity on a variety of substrates, including polydimethylsiloxane (PDMS), using EHD printing. But in general, extending printed electronics from rigid or flexible substrates to stretchable substrates face challenges from the interaction between functional inks and substrates.²¹ The surface tension and wettability of the ink have been investigated as factors for printing performance. ³⁹ Surface properties of substrate is the other key factor. Most stretchable substrates are made up of low-surface energy polymers. For example, PDMS is one of the most widely used materials in stretchable electronics. However, the low surface free energy of PDMS (21 - 25 mJ·m⁻²)⁴⁰ results in relatively poor intrinsic wettability between PDMS and functional inks. A few chemical and mechanical surface modification approaches, such as corona discharges,⁴¹ plasma treatment,⁴² UV-Ozone (UVO) treatment⁴³⁻⁴⁵ and dopamine coating⁴⁶ have been used to modify the surface energy of PDMS and thus enhance the wettability between the

inks and the substrate. The chemical approaches include corona discharge, plasma treatment, and UVO treatment of PDMS, while the physical approaches rely on coating of different materials on top of PDMS surface. Here we select UVO treatment and polydopamine treatment (coating) as two representative chemical and physical methods, respectively. More specifically, UVO treatment is widely used, relatively mild and not causing severe surface cracking as in other methods like plasma treatment. Polydopamine, as a biocompatible coating material, can strongly adhere to a variety of substrates. Dopamine can be self-assembled on PDMS surface to form a stable hydrophilic coating layer without changing mechanical properties of PDMS. However, the effect of these surface modifications on EHD printing, especially of AgNWs, has not been well investigated. In this work, we explore the use of surface modification for printed stretchable electronics, using AgNWs and PDMS as the representative conducting ink material and substrate, respectively.

Herein, we systematically study the effect of two surface modification methods of the PDMS substrate, UVO treatment and dopamine coating, on the EHD printing behavior of conductive AgNW inks. First, the dynamic contact angles between ink and PDMS with different treatment time (i.e. dose) were measured and analyzed for both UVO and dopamine treatments. Contact angle hysteresis (CAH) were calculated to obtain an insight into the mechanism of surface modification. Then, the hydrophobic stability of the UVO and dopamine treated substrates was studied to achieve the best surface modification with a long shelf life. Linewidth, edges roughness, pattern thickness and sheet resistance of printed patterns were measured to study the quality of the printed patterns. With the facile surface modification strategy, diversiform patterns could be achieved by not only adjusting the printing parameters but also distinguishing surface treatment doses. Furthermore, a complex conductive pattern printed on PDMS was integrated into an

electrical circuit with LED light and power source to demonstrate its application in stretchable wearable devices. While the two treatments of PDMS and their effect on the water contact angles have been studied before, to our knowledge this is the first report on their effect on the contact angles of AgNW/ polyethylene oxide (PEO) ink and the printing performances.

2. Experimental Section

Preparation of AgNW/PEO ink: AgNWs were synthesized by the modified polyol process⁴⁷ with an average diameter of ~120 nm and an average length of ~20 μm. After synthesis, the AgNWs were suspended in ethanol for ink preparation. The PEO powder (Mv: 1 000 000) (Sigma-Aldrich) was first diluted in DI water to form a clear solution. Then the 4 wt% PEO solution was mixed with the AgNWs to form the conductive AgNW ink with 25 mg·ml⁻¹ AgNW concentration. The ink with 4% wt PEO and 25 mg/mL AgNWs in the liquid phase has a conductivity of 0.11S/cm. Preparation and surface modification of PDMS substrate: PDMS was prepared using the Sylgard 184 Silicone Elastomer Kit by mixing the base and curing agent with a typical mass ratio of 10:1. After mixing, liquid PDMS was degassed in vacuum to remove air bubbles and then spincoated on a glass slide to form a thin film, which was cured at 80 °C for 3 h. The UVO treatment of PDMS surfaces was performed in a commercial UVO chamber (Jelight Company, Inc., Model 42A with output power of 28 mW·cm⁻²). When treated, the PDMS films were exposed to shortwavelength UV radiation, mainly at 184.9 nm and 253.7 nm. To achieve PDMS substrates with different UVO treatment, an Ecoflex film was used as a mask to selectively block UVO exposure for certain region, so as to obtain a PDMS film with several regions with different amounts of UVO exposure time. For dopamine coating, a PDMS substrate was immersed in a dilute aqueous dopamine solution with 2 mg dopamine per ml of 10 mM tris-HCl with a pH value of 8.5. After

specified immersion time, the PDMS substrate was taken out from the solution and blow-dried. To achieve PDMS substrates with different amounts of treatment time across the substrate, an additional PDMS film was used as a mask to cover select regions of the PDMS substrate during the immersion process.

Contact angle measurement: The sessile drop technique was utilized to measure the advancing and receding contact angles of the ink on a PDMS substrate with different amounts of UVO exposure time (from 5 min to 60 min) or dopamine coating time (from 1 min to 60 min). In all the measurement, AgNW/PEO ink was used as the probe liquid, and a contact angle microscope (Ramé-hart Instrument Co., Model 200-U1) was used to measure the contact angle at room temperature. The volume of measured ink droplet was 5 μ L. The flow rate was 1 μ L/s for measuring advancing contact angles and 0.5 μ L/s for measuring receding contact angles. The needle used to add or withdraw ink was a standard 22-gauge needle. The advancing and receding contact angles (θ _A and θ _R) were measured on both sides of the drop at five different locations for each sample. After different amounts of aging time (5 - 120 min), θ _A and θ _R were measured again at five different locations for each sample to evaluate the hydrophobic stability of the surface treatment.

EHD Printing: The EHD printing system includes three sub-systems: a pneumatic dispensing system, a voltage supply system, and a precision three-axis translation stage. Patterns were first created in CAD software and then converted to the program code for printing. A nozzle with an inner diameter of 150 μm and an outer diameter of 250 μm was used for EHD printing. The printing voltage was selected to be 1500 V, and the back pressure was 0.4 psi. Printing speed varied from 1–10 mm·s⁻¹ to print features with different linewidths. In this work, the stable cone-jet mode or direct writing mode of EHD printing was used to print the AgNW ink onto the substrate, in which

a continuous jet was ejected from the Taylor cone for the ink transfer. During the printing process, the ink was continuously printed through a stream of ink onto the substrate, and the feature was defined by moving the substrate in a pre-programmed pattern. After printing, the printed AgNW patterns were soaked in DI water for 30 seconds to remove PEO, and then dried in an oven at 50 °C. This post-processing process was repeated several times to improve the conductivity of the printed samples.

Sheet resistance and thickness measurements: To obtain the sheet resistance of each printed line, a 4-probe method was used to measure the resistance (R) of these printed lines. Rs was calculated by Rs=RW/L, where W and L are the width and measured length (set as 10 mm when tested) of the lines, respectively. The thickness (t) of the printed lines was measured by Confocal Laser Scanning Microscope (Keyence VKx1100). Based on the measured average thickness t, the electrical conductivity σ can be calculated by $\sigma = L/(R \times t \times W)$.

3. Results and Discussion

For EHD printing, the wetting property of an ink on a substrate plays a significant role in printability and printing resolution. Untreated PDMS is hydrophobic with low surface energy, leading to poor wetting of the AgNW/PEO ink on PDMS. The ink cannot settle well on the PDMS surface to form continuous patterns. Thus, surface modification that can change the PDMS surface from hydrophobic to hydrophilic is a prerequisite to enable reliable EHD printing. The two surface modification approaches for PDMS in this work, UVO treatment and dopamine coating, have different surface wettability enhancing mechanisms. For UVO treatment, an oxidation-induced silica-like layer of several to hundreds of nanometers in thickness is formed, which enhances the adhesion between PDMS and other polar agents in inks. For dopamine coating, the dopamine coated on PDMS surface is oxidized in air and polymerizes, resulting in a polydopamine thin layer

on the PDMS surface. The catechol groups in polydopamine have strong interaction with various functional groups to enhance the adhesion between them. The surface treatment of PDMS using both approaches and the EHD direct printing with cone-jet mode is schematically illustrated in Figure 1.

3.1. Dynamic Contact Angles

The contact angle is conventionally measured to quantify the wettability of a liquid on a solid surface. To study the dynamic ink-substrate interaction, dynamic contact angles need to be studied, including advancing contact angle, θ_A , and receding contact angle, θ_R . The advancing contact angle, θ_A , is measured when the contact area between the liquid and the solid increases, while the receding contact angle θ_R is when that decreases. Both the advancing and receding contact angles can affect the EHD printing process. At the beginning of the EHD printing process, the ink meniscus and a cone shape from the meniscus are formed, and the ink is extruded from the nozzle to the substrate, thus θ_A is essential. When the ink is deposited to the substrate as the stage moves, the ink settlement on the substrate is largely affected by θ_R . Both contact angles are important to characterize the wettability of an ink on a substrate.

The optical images of the dynamic contact angles of AgNW/PEO ink on (i) untreated PDMS, (ii)15 min dopamine treated PDMS and (iii)30 min UV treated PDMS are shown in Figure 2a, exhibiting enhanced wettability after treatment. θ_A and θ_R of the untreated PDMS were measured to be 113.7° and 76.4°, respectively. Figure 2b shows measured θ_A and θ_R of Ag NW/PEO ink on UVO-treated PDMS substrate as a function of UVO treatment time, with all the angles measured immediately after the treatment. It can be observed that as the UVO treatment time increased, the originally hydrophobic PDMS substrate gradually became hydrophilic. Both θ_A and θ_R decreased significantly with time when the UVO treatment was less than 30 min, and then became relatively

stable with further exposure. Figure 2c shows the measured θ_A and θ_R of AgNW/PEO ink on polydopamine coated PDMS substrate as a function of soaking time. θ_A and θ_R decreased as the dopamine treatment time increased. θ_R became relative stable when the treatment time was over 10 min, while θ_A decreased continuously with increasing treatment time. The stable θ_A and θ_R , especially θ_{A} , of the dopamine coated PDMS were larger than those of the UVO treated PDMS. Besides the contact angles, the contact angle hysteresis (CAH) was also studied to evaluate the surface uniformity at different treatment conditions. CAH is the difference between the advancing and the receding contact angle. It is widely recognized that topographical or chemical heterogeneity of the substrate is the main sources of CAH. 48 More specifically, the larger the surface roughness and/or higher molecular mobility, the higher the CAH. Figure 2d illustrates the CAH as a function of the UVO and dopamine treatment time. The initial increase of CAH for UVO treated substrates indicates that the surface becomes more heterogeneous, which can be attributed to the surface change caused by chain scission reaction.⁴¹ It is known that the advancing and receding angles are more associated with the low and high surface energy regions on a heterogeneous polymer surface, respectively. 49 In the first 15-20 min of treatment, the surface of PDMS is only partially oxidized and the oxidized region (with higher surface energy) contributes to the significant drop of θ_R (red curve in Figure 2b). The reduced CAH for longer exposure time from 20 to 30 min could come from formation of a cross-linked silica-like structure, which can enhance the wettability with ink due to the increased O/Si ratio on the surface. Complete surface oxidation occurs during this time, which leads to the rapid drop of θ_A (black curve in Figure 2b), owing to vanishing of the low surface energy regions. For 30 min and longer, the CAH trended to be steady at a low value, indicating presence of a homogeneous surface consisting completely of the silica-like structure. It could be speculated that the UVO treated substrate can become printable

when the treatment time is around 30 min. For the dopamine treated substrates, printability depended on whether there was enough polydopamine film formed. The CAH showed a trend of rising first and then slightly decreasing. The initial rapid increase is because of the surface heterogeneity caused by the partially coated polydopamine. As can be seen in Figure S1a, the treated surface of PDMS showed homogeneous morphology when the treatment time was 8 minutes. With the soaking time increasing, the agglomerations grew due to the self-polymerization and aggregation of polydopamine molecules, ⁵⁰ as shown in Figure S1b-e. When the soaking time was beyond 20 minutes, the CAH slightly decreased and became steady at a higher value than that of the UVO treated substrates. As shown in Figure S1c-e, longer treatment time caused deposition of thicker layer of polydopamine attributed to the continuous intermolecular interactions. ⁵⁰⁻⁵² The film gradually covered the pristine PDMS completely and lead to the slightly dropping of CAH when treatment time was beyond 20 minutes. It can be speculated that the polydopamine film may not completely cover the PDMS surface from 8 minutes treatment to 15 minutes treatment, where an obvious contact angle hysteresis change was detected. It is worth noting that the dynamic contact angle of dopamine treated surface started to be steady when soaking 10 min, while CAH was steady from 20 min. We believe that the dopamine treated surface only need a partially covered polydopamine layer to be wettable with the ink.

3.2. Hydrophobic Stability

In addition to the immediate effect of the two treatments, stability of the treatments is also important for the EHD printing as it determines the shelf life of the treated samples. Although the UVO treatment is effective in modifying the PDMS films from hydrophobic to hydrophilic, many studies have reported hydrophobic recovery after UVO treatment, indicating a reversing trend of the surface properties after treatment. The hydrophobic stability of the UVO and dopamine treated

PDMS samples was evaluated by measuring their θ_A and θ_R of after different amounts of aging time (5 to 120 min) after the treatments. The results are shown in Figure 3a and Figure 3b.

For UVO treatment, all the samples illustrated certain level of hydrophobic recovery. For a small dose of UVO treatment (i.e., exposure time < 20 min), θ_A and θ_R of the PDMS samples exhibited small changes as the aging time increased (Figure 3a). Oláh et al. have suggested that lower doses of UVO treatment can result in gradual formation of a liquid-like layer, consisting of free oligomeric PDMS on top of the partly oxidized PDMS surface. 45 The hydrophobic recovery in this case is due to reorientation of the polar groups formed by the partial oxidation.⁵³ Figure 3c shows that the CAH only changed slightly with the increasing aging time, indicating that the surface heterogeneity is nearly unchanged, because no silica-like structure is formed. On the other hand, higher dose UVO treatment (i.e., exposure time > 30 min) resulted in significant hydrophobic recovery. The treated surfaces exhibited a rapidly increasing hydrophobicity with the increasing aging time. The dominating mechanism for this hydrophobic recovery is believed to be the changes of the surface homogeneity; more specifically, migration of siloxanes to the surface reduces the homogeneity of the silica layer. The dominant mechanism for this hydrophobic recovery is believed to be the change of the surface homogeneity; more specifically, migration of siloxanes to the surface reduces the homogeneity of the silica layer, shown schematically in Figure 3c. This mechanism is supported by the CAH results. The CAH increased significantly as a function of the aging time for the treatment time over 30 min, as shown in Figure 3d, which confirms that the surface changes from being homogeneous to heterogeneous. Based on the results shown in Figure 3a, the effect of hydrophobic recovery was stabilized after about 90 min. Accordingly, the UVO treated samples should be used for printing 2 hours after treatment to ensure that the surface properties were stabilized.

Dopamine-coated samples showed no evident hydrophobic recovery. For example, for a PDMS substrate that was treated for 15 min in dopamine solution, Figure 3b shows the nearly constant contact angles irrespective of the aging time, indicative of the hydrophobic stability. The CAH results from Figure 3c also show that there was no apparent change in the surface heterogeneity during aging. To summarize, the dopamine coating can maintain the hydrophobic stability of the treated samples, while the UVO treatment needs to be optimized to in terms of the treatment time considering both the required hydrophobicity for printing and the shelf life of the treated samples.

3.3. Effect of Treatment on EHD Printing

For EHD printing, printed resolution is reduced on highly hydrophilic substrates due to ink spreading, while the ink is difficult to settle on highly hydrophobic substrates, leading to nonuniform and/or discontinuous features. In this study, conductive AgNW lines were printed on the PDMS substrate with different amounts of UVO or dopamine treatment time in order to identify the optimal treatment time for EHD printing with respect to the linewidth and conductivity. The scanning electron microscope (SEM) images of printed AgNW patterns with percolated network at different magnification are shown in Figure S2. These conductive lines were also printed at different printing speeds to study the effect of the speed on the resulting linewidth. In general, the printed linewidth decreases as the printing speed increases (Figure 4a and 4b), while too high the printing speed can result in discontinuous lines (> 10 mm s⁻¹). Due to the ink spreading and wetting on the treated PDMS, the printed lines were wider than the diameter of jet and can be even wider than the inner diameter of the nozzle at a low printing speed.

In the case of UVO treatment, all the PDMS substrates were rested for 2 hours after UVO exposure, to ensure the surface stabilized after hydrophobic recovery. When the exposure time was short (< 20 min), the ink had poor wettability to the PDMS surface, as evidenced by the relatively large

contact angles. Thus the printed line exhibited poor uniformity and discontinuity. As shown in Figure S3a, the printed lines were rough and irregular when the PDMS surface was exposed to UVO for 10 min. When the exposure time was long (> 40 min), the contact angle was still large after certain aging time due to the hydrophobic recovery, which again resulted in poor printing performance. After considering the tradeoff between hydrophilicity and hydrophobic recovery, the feasible UVO treatment range was from 20-40 min. Figure 4a shows the linewidth as a function of the printing speed (from 1 to 10 mm s⁻¹) under intermediate of UVO exposure time (from 20 to 40 min). The 20-minute UVO treatment resulted in most of the surface to be oxidized, which is enough for printing. Longer treatment time led to hydrophobic recovery, while the hydrophobic recovery was moderate for 30-min and 40-min treatment. After hydrophobic recovery, the contact angle of 30-min treatment was smaller than that of 40-min. That is, the surface treated by 30 min was more hydrophilic and the linewidth of the printed lines at the same speed was wider. The linewidth (or resolution) was also affected by the printing speed. In the speed range in this study (1 to 10 mm s⁻¹), higher printing speed resulted in smaller linewidth (and better resolution). In the case of dopamine treatment, when the PDMS was treated less than 8 min, continuous lines could not be printed on, as shown in Figure S3b, consistent with the large dynamic contact angles at this condition. When the dopamine treatment time was long enough (more than 15 min), the plot of CAH drops slightly and then tends to relatively stabilize. While, the printed linewidth is only slightly affected by the increased treatment time, as shown by the linewidths as a function of the printing speed for 30 min, 45 min and 60 min dopamine treatment in Figure S4. We believe that after PDMS treated more than 15 min, increasing treatment time contributes to the thicker polydopamine film, which does not enhance the wettability of AgNW ink on the treated PDMS surface significantly. Then, we chose the dopamine treatment time from 8 to 15 min to study their effect on EHD printing (Figure 4b). At the same printing speed, the linewidth increased as the dopamine treatment time increased. With the same dopamine treatment time, the linewidth decreased as the printing speed increases. In this work, the shortest proper dopamine treatment time for EHD printing was 8 min, and the narrowest linewidth obtained in this situation was around 50 μm. The optical microscopy image of the printed conductive lines with the highest resolution of ~50 μm is shown in Figure 4c. The printing of 1D nanomaterials, such as AgNWs, are very challenging and different from the printing of nanoparticle-based inks and solvent-based inks. Considering the length of the AgNWs (~20μm) in this work and the inevitable random distribution of the AgNW orientation in the printing lines, the 50-μm line width represents excellent resolution for the traditionally hard-to-printing AgNWs.

3.4. Characterization of Printed Conductors

The morphology and electrical properties of the printed patterns are of important relevance to the device performances. 30 min UVO and 15 min dopamine treatments of PDMS were chosen for printing AgNW conductive lines for subsequent evaluation of morphology and electrical conductivity. AgNW lines were printed at different printing speeds and then their width, thickness, and resistance were measured, as shown in Figure 5. Compared to the 30 min UVO treatment (defined as UVO-30), the 15 min dopamine treatment (defined as Dopamine-15) resulted in printed lines with better uniformity, higher resolution and lower line edge roughness, as shown in the optical images in Figure 5a and b. Here the root mean square (RMS) line edge roughness (LER) is a way to characterize the uniformity of printed lines, defined by the variation in the position of the edge of a line. The edges of line were detected by a NIH public domain software, Image J. Then the RMS LER, calculated by the plugin AnalyzeStripes, is plotted in Figure 5c as a function of the printing speed. It can be seen that Dopamine-15 led to very low edge roughness, while UVO-

30 does much higher edge roughness, especially at the small printing speeds. The rough edges may be caused by the nonuniform distribution of low and high energy region due to hydrophobic recovery of the PDMS surface. Figure 5d and e show the line thicknesses before and after post-processing (i.e., water soaking) at different printing speeds for UVO-30 and Dopamine-15, respectively. The line thickness decreased with the increase of the printing speed in both cases due to the reduction of the loaded ink at a higher speed. Moreover, although the line thickness before post-processing was comparable between UVO-30 and Dopamine-15, they dropped markedly after post-processing for UVO-30, which indicates that more AgNWs might be washed away in this case, resulting a lower loading density of AgNWs in case of UVO-30. The detailed confocal microscopy images and thickness profiles of the printed lines for both UVO-30 and Dopamine-15 (printing speed: 4 mm·s⁻¹) can be found in Figure S5.

After post-processing, the printed patterns became conductive, and the sheet resistance and conductivity were measured and calculated. As shown in Figure 5f and g, for both UVO-30 and Dopamine-15, the sheet resistance increases monotonically with the increasing printing speed. Compared to Dopamine-15, UVO-30 resulted in higher sheet resistance at the same printing speed. The lowest sheet resistance obtained in this work was $0.14 \Omega/\Box$ for Dopamine-15 at the printing speed of 1 mm·s⁻¹. The sheet resistance obtained in our work is the lowest for one-run printed AgNWs among the reported works, to the best of our knowledge. The conductivity of the printed patterns is also shown in Figure 5f and g. As expected, the conductivity decreased with the increasing printing speed and UVO-30 showed much lower conductivity than Dopamine-15 at all the printing speeds. The reduced loading density of AgNWs decreased the conductivity of these printed lines. According to Rs = $1/t\sigma$, both the lower conductivity and the lower thickness of the

patterns contributed to the high sheet resistance for UVO-30. To summarize, the printed lines for UVO-30 (which has a higher wettability from smaller contact angle) showed larger linewidth and lower thickness with higher line edge roughness, while the printed lines for Dopamine-15 provided high-resolution features with smaller linewidth, higher thickness, and smoother line edges.

To test the stretchability and flexibility of printed patterns on treated PDMS, bending and stretching tests were performed. The samples were clamped on a motorized stage that can provide continuous bending and tensile strain of the sample. The resistance of the samples at different stretching and bending levels was measured by a multimeter in real-time. Figure S6a shows the tensile test results. The conductor printed on the UVO and dopamine treated PDMS can both endure the strain over 20%. Figure S6b shows the bending test results of the printed horseshoe pattern on dopamine-15 and UVO-30 substrate. Even when the bending curvature radius was reduced to about 1 mm, the maximum resistance changes were still under 4%. Overall, the resistance changes of the printed conductor on UVO treated PDMS were slightly larger in both tensile and bending tests, since the thickness of the printed AgNWs on UVO treated PDMS was thinner (Figure 5d-e). For the cyclical bending tests, the resistance of the printed conductor on dopamine treated PDMS remain unchanged after 500-cycle bending tests with a bending radius at 1 mm (Figure S6c), while the resistance on UVO treated PDMS changes slightly (around 1%) after 500 cycles (Figure S6d).

3.5 Demonstration of EHD Printing for Device Fabrication

After surface treatment, complex patterns (e.g., fractal patterns⁵¹) can be directly printed on the PDMS substrates using EHD printing, which is a critical enabling step for device fabrication. As learned above, both the surface treatment and printing speed can be used to regulate the printing results of the AgNW/PEO ink, such as linewidth. To visualize the effect of the printing speed, two

PDMS substrates, one each treated 15 min by dopamine and 30 min by UVO, were used. A continuous Peano curve was printed on the dopamine-treated PDMS substrate, with the printing speed switching from 1 to 4 mm · s⁻¹ during the printing process without stop (Figure 6a); similarly, another Peano curve on the UVO-treated PDMS substrate, with the printing speed from 2 to 6 mm·s⁻¹ (Figure S7). Clearly different linewidths were obtained at different printing speeds. To visualize the effect of the surface treatment time, different regions of the same PDMS substrate were treated with different amounts of time and then a feature was printed across the regions. For example, a Peano curve was printed on a dopamine treated PDMS substrate with two regions, one treated by 7 min and the other by 15 min. The Peano curve printed on the 7 min treated region was not as uniform as that on the 15 min region, as shown in Figure 6b. For the UVO treatment, the PDMS substrate was divided into four regions, each treated differently by 5, 10, 15, and 30 min. As shown in Figure 6c, only the properly treated region (i.e., with 30 min UVO exposure) had the suitable wettability and was printable with continuous features. Due to the poor wettability caused by insufficient surface oxidation in regions of 5 minutes, 10 minutes, and 15 minutes treatment, continuous features cannot be printed onto the surface of these regions.

The performance of the printed AgNWs conductor under bending and stretchability tests has been systematically studied in our previous research³³. Excellent stretchability with stable resistance response was achieved from the experiments. In this work, complex custom-designed patterns can be reliably printed onto properly treated PDMS surface for device fabrication. A fractal pattern of Sierpinski square was printed on a thin PDMS film using the AgNW/PEO ink and sealed by a thin top layer of PDMS after post-processing, for wearable electronics applications (Figure 6d). In the fractal pattern, the sharp corners were rounded from the mathematically defined fractal layout to improve the elastic mechanics. A PDMS film with 15 min dopamine treatment

was chosen as the substrate here, due to its overall superior printing performances (e.g., low edge roughness, high uniformity, and high electric conductivity).

A light-emitting diode (LED) was connected to the AgNW Sierpinski pattern. The thin patch electronics can be easily attached to the skin or other curved objects. As shown in Figure 6e, the thin patch was wrapped around the fingertip, maintaining its electronic functionality under bending, and the Sierpinski square patterned conductor can endure 200 cycles bending test at the 8 mm curvature radius (Figure S8). Figure 6f shows that when the thin patch was attached to the wrist, the LED lighting remained unchanged during wrist bending forward and backward, indicating that the thin patch electronics can also undergo tension and compression associated with the wrist bending.

4. Conclusion

In summary, we reported a systematic investigation on two surface modification methods, UVO treatment and polydopamine coating, on PDMS for high-resolution and scalable EHD printing of AgNW patterns. The advancing and receding contact angles were reduced by both modification methods. We investigated the effect of treatment time and aging time (hydrophobic recovery) on the EHD printing performances including morphology (linewidth, thickness, and edge roughness) and electric conductivity. We found that the proper treatment time (20 to 40 min for UVO and 8 to 15 min for dopamine) is critical to ensure high-resolution and reliable EHD printing. The dopamine-coated PDMS surfaces showed better resolution and lower line edge roughness than the UVO-treated PDMS surfaces. The UVO-treatment can also provide decent resolution, thus find its own applications, as it provides a simple dry treatment method that can potentially be applied to a large area at low cost. Enhanced by the surface modification, complex patterns can be reliably printed, with a resolution as high as 50 μm. With the facile surface modification strategy,

distinguishing surface treatment doses. A fractal-inspired pattern, Sierpinski curve, was printed on modified PDMS surface and integrated into an electrical circuit with LED light and power source to demonstrate its application in stretchable wearable devices. The reported results on the surface modification methods can be extended to other types of elastomeric substrates, paving the way for high-resolution and scalable printing of nanomaterials for flexible and stretchable electronics.

ASSOCIATED CONTENT

Supporting Information

Supporting Information is available online.

The scanning electron microscope (SEM) images of the surface of polydopamine treated PDMS; The SEM images of printed AgNWs, Printed lines with non-ideal treatment dose; More results of linewidths with different dopamine treatment time; Details of thickness measurement of printed lines; Tensile and bending test of horseshoe patterned AgNW; Peano curve printed on UVO treated PDMS; Cyclic bending test of Serpensiki patterned conductor.

AUTHOR INFORMATION

Corresponding Author

- 1. Jingyan Dong Department of Industrial and Systems Engineering, North Carolina State University, Raleigh, North Carolina 27606, USA
- 2. Yong Zhu Department of Mechanical and Aerospace Engineering, North Carolina State University, Raleigh, NC 27695, USA

Author

Ping Ren – Department of Industrial and Systems Engineering, North Carolina State Unicersity, Raleigh, North Carolina 27695, USA

Yuxuan Liu – Department of Mechanical and Aerospace Engineering, North Carolina State University, Raleigh, North Carolina 27695, USA

Runqiao Song – Department of Mechanical and Aerospace Engineering, North Carolina State University, Raleigh, NC 27695, USA

Author Contributions

Ping Ren and Yuxuan Liu contribute equally to this paper.

Notes

The authors declare no competing financial interest.

ACKNOWLEDGMENT

The authors gratefully acknowledge the financial support from the National Science Foundation (NSF) through Award No. CMMI-1728370.

REFERENCES

- 1. Kim, H. W.; Kim, T. Y.; Park, H. K.; You, I.; Kwak, J.; Kim, J. C.; Hwang, H.; Kim, H. S.; Jeong, U., Hygroscopic Auxetic On-Skin Sensors for Easy-to-Handle Repeated Daily Use. *ACS Appl. Mater. Interfaces* **2018**, *10* (46), 40141-8.
- 2. Liu, Y.; He, K.; Chen, G.; Leow, W. R.; Chen, X., Nature-Inspired Structural Materials for Flexible Electronic Devices. *Chem. Rev.* **2017**, *117* (20), 12893-941.
- 3. Rogers, J. A.; Chen, X.; Feng, X., Flexible Hybrid Electronics. *Adv. Mater.***2020**, *32* (15), 1905590.
- 4. Kaltenbrunner, M.; Sekitani, T.; Reeder, J.; Yokota, T.; Kuribara, K.; Tokuhara, T.; Drack, M.; Schwodiauer, R.; Graz, I.; Bauer-Gogonea, S.; Bauer, S.; Someya, T., An Ultralightweight Design for Imperceptible Plastic Electronics. *Nature* **2013**, *499* (7459), 458-63.

- 5. Xu, S.; Zhang, Y.; Cho, J.; Lee, J.; Huang, X.; Jia, L.; Fan, J. A.; Su, Y.; Su, J.; Zhang, H.; Cheng, H.; Lu, B.; Yu, C.; Chuang, C.; Kim, T. I.; Song, T.; Shigeta, K.; Kang, S.; Dagdeviren, C.; Petrov, I.; Braun, P. V.; Huang, Y.; Paik, U.; Rogers, J. A., Stretchable Batteries with Self-similar Serpentine Interconnects and Integrated Wireless Recharging Systems. *Nat. Commun* **2013**, *4*, 1543.
- 6. Gao, L.; Zhang, Y.; Zhang, H.; Doshay, S.; Xie, X.; Luo, H.; Shah, D.; Shi, Y.; Xu, S.; Fang, H.; Fan, J. A.; Nordlander, P.; Huang, Y.; Rogers, J. A., Optics and Nonlinear Buckling Mechanics in Large-Area, Highly Stretchable Arrays of Plasmonic Nanostructures. *ACS Nano* **2015**, *9* (6), 5968-75.
- 7. Rogers, J. A.; Someya, T.; Huang, Y., Materials and Mechanics for Stretchable Electronics. *Science* **2010**, *327* (5973), 1603-7.
- 8. Jeong, J. W.; Yeo, W. H.; Akhtar, A.; Norton, J. J.; Kwack, Y. J.; Li, S.; Jung, S. Y.; Su, Y.; Lee, W.; Xia, J.; Cheng, H.; Huang, Y.; Choi, W. S.; Bretl, T.; Rogers, J. A., Materials and Optimized Designs for Human-machine Interfaces via Epidermal Electronics. *Adv. Mater.* **2013**, *25* (47), 6839-46.
- 9. Kim, J.; Banks, A.; Cheng, H.; Xie, Z.; Xu, S.; Jang, K. I.; Lee, J. W.; Liu, Z.; Gutruf, P.; Huang, X.; Wei, P.; Liu, F.; Li, K.; Dalal, M.; Ghaffari, R.; Feng, X.; Huang, Y.; Gupta, S.; Paik, U.; Rogers, J. A., Epidermal Electronics With Advanced Capabilities in Near-Field Communication. *Small* **2015**, *11* (8), 906-12.
- 10. Lee, H.; Song, C.; Hong, Y. S.; Kim, M. S.; Cho, H. R.; Kang, T.; Shin, K.; Choi, S. H.; Hyeon, T.; Kim, D. H., Wearable/Disposable Sweat-Based Glucose Monitoring Device with Multistage Transdermal Drug Delivery Module. *Sci. Adv.* **2017**, *3* (3), 1601314.

- 11. Son, D.; Lee, J.; Qiao, S.; Ghaffari, R.; Kim, J.; Lee, J. E.; Song, C.; Kim, S. J.; Lee, D. J.; Jun, S. W.; Yang, S.; Park, M.; Shin, J.; Do, K.; Lee, M.; Kang, K.; Hwang, C. S.; Lu, N.; Hyeon, T.; Kim, D. H., Multifunctional Wearable Devices for Diagnosis And Therapy of Movement Disorders. *Nat. Nanotechnol.* **2014**, *9* (5), 397-404.
- 12. Lee, H.; Choi, T. K.; Lee, Y. B.; Cho, H. R.; Ghaffari, R.; Wang, L.; Choi, H. J.; Chung, T. D.; Lu, N.; Hyeon, T.; Choi, S. H.; Kim, D. H., A Graphene-Based Electrochemical Device with Thermoresponsive Microneedles for Diabetes Monitoring and Therapy. *Nat. Nanotechnol.* **2016**, *11* (6), 566-72.
- 13. Xie, Z.; Avila, R.; Huang, Y.; Rogers, J. A., Flexible and Stretchable Antennas for Biointegrated Electronics. *Adv. Mater.***2020**, *32* (15), 1902767.
- 14. Yao, S.; Swetha, P.; Zhu, Y., Nanomaterial-Enabled Wearable Sensors for Healthcare. *Adv. Healthc. Mater.* **2018,** *7* (1), 1700889.
- 15. Amjadi, M.; Pichitpajongkit, A.; Lee, S.; Ryu, S.; Park, I., Highly Stretchable and Sensitive Strain Sensor Based on Silver Nanowire-Elastomer Nanocomposite. *ACS Nano* **2014**, *8* (5), 5154-63.
- 16. Lipomi, D. J.; Vosgueritchian, M.; Tee, B. C.; Hellstrom, S. L.; Lee, J. A.; Fox, C. H.; Bao, Z., Skin-Like Pressure and Strain Sensors Based on Transparent Elastic Films of Carbon Nanotubes. *Nat. Nanotechnol.* **2011**, *6* (12), 788-92.
- 17. Yao, S.; Ren, P.; Song, R.; Liu, Y.; Huang, Q.; Dong, J.; O'Connor, B. T.; Zhu, Y., Nanomaterial-Enabled Flexible and Stretchable Sensing Systems: Processing, Integration, and Applications. *Adv. Mater.* **2020**, *32* (15), e1902343.

- 18. Liang, J.; Li, L.; Tong, K.; Ren, Z.; Hu, W.; Niu, X.; Chen, Y.; Pei, Q., Silver Nanowire Percolation Network Soldered with Graphene Oxide at Room Temperature and its Application for Fully Stretchable Polymer Light-Emitting Diodes. *ACS Nano* **2014**, *8* (2), 1590-600.
- 19. Gong, S.; Yap, L. W.; Zhu, B.; Cheng, W., Multiscale Soft-Hard Interface Design for Flexible Hybrid Electronics. *Adv. Mater.* **2020**, *32* (15), 1902278.
- 20. Sim, K.; Rao, Z.; Ershad, F.; Yu, C., Rubbery Electronics Fully Made of Stretchable Elastomeric Electronic Materials. *Adv. Mater.***2020**, *32* (15), 1902417.
- 21. Huang, Q.; Zhu, Y., Printing Conductive Nanomaterials for Flexible and Stretchable Electronics: A Review of Materials, Processes, and Applications. *Adv. Mater. Technol* **2019**, *4* (5), 1800546.
- 22. He, B.; Yang, S.; Qin, Z.; Wen, B.; Zhang, C., The Roles of Wettability and Surface Tension in Droplet Formation During Inkjet Printing. *Scientific Reports* **2017**, 7 (1), 11841.
- 22. Yao, S.; Zhu, Y., Nanomaterial-Enabled Stretchable Conductors: Strategies, Materials and Devices. *Adv. Mater.* **2015**, *27* (9), 1480-511.
- 23. Xu, F.; Zhu, Y., Highly Conductive and Stretchable Silver Nanowire Conductors. *Adv. Mater.* **2012**, *24* (37), 5117-22.
- 24. Lee, P.; Lee, J.; Lee, H.; Yeo, J.; Hong, S.; Nam, K. H.; Lee, D.; Lee, S. S.; Ko, S. H., Highly Stretchable and Highly Conductive Metal Electrode by Very Long Metal Nanowire Percolation Network. *Adv. Mater.* **2012**, *24* (25), 3326-32.
- 25. Huang, Q.; Zhu, Y., Gravure Printing of Water-based Silver Nanowire ink on Plastic Substrate for Flexible Electronics. *Sci. Rep.* **2018**, *8* (1), 15167.

- 26. Onses, M. S.; Sutanto, E.; Ferreira, P. M.; Alleyne, A. G.; Rogers, J. A., Mechanisms, Capabilities, and Applications of High-Resolution Electrohydrodynamic Jet Printing. *Small* **2015**, *11* (34), 4237-66.
- 27. Li, X.; Park, H.; Lee, M. H.; Hwang, B.; Kim, S. H.; Lim, S., High Resolution Patterning of Ag Nanowire Flexible Transparent Electrode via Electrohydrodynamic Jet Printing of Acrylic Polymer-Silicate Nanoparticle Composite Overcoating Layer. *Org. Electron* **2018**, *62* (62), 400-6.
- 28. Meng, Z.; He, J.; Xia, Z.; Li, D., Fabrication of Microfibrous PCL/Mwcnts Scaffolds via Melt-Based Electrohydrodynamic Printing. *Materials Letters* **2020**, *278*.
- 29. Alzakia, F. I.; Jonhson, W.; Ding, J.; Tan, S. C., Ultrafast Exfoliation of 2D Materials by Solvent Activation and One-Step Fabrication of All-2D-Material Photodetectors by Electrohydrodynamic Printing. *ACS applied materials & interfaces* **2020**, *12* (25), 28840-28851.
- 30. Lei, Q.; He, J.; Li, D., Electrohydrodynamic 3D Printing of Layer-Specifically Oriented, Multiscale Conductive Scaffolds for Cardiac Tissue Engineering. *Nanoscale* **2019**, *11* (32), 15195-15205.
- 31. Han, Y.; Dong, J., Electrohydrodynamic (EHD) Printing of Molten Metal Ink for Flexible and Stretchable Conductor with Self-Healing Capability. *Adv. Mater. Technol* **2018**, *3* (3), 1700268.
- 32. Han, Y.; Dong, J., Design, Modeling and Testing of Integrated Ring Extractor for High Resolution Electrohydrodynamic (EHD) 3D Printing. *J Micromech Microeng* **2017**, *27* (3), 035005.
- 33. Prasetyo, F. D.; Yudistira, H. T.; Nguyen, V. D.; Byun, D., Ag Dot Morphologies Printed Using Electrohydrodynamic (EHD) Jet Printing Based on a Drop-on-Demand (DOD) Operation. *J of Micromech Microeng* **2013**, *23* (9), 095028.

- 34. Xu, W.; Zhang, S.; Xu, W., Recent Progress on Electrohydrodynamic Nanowire Printing. *Sci. China Mater.* **2019**, *62* (11), 1709-1726.
- 35. Liu, L.; Cui, B.; Xu W.;, Ni, Y.; Zhang, S.; Xu, W., Highly aligned indium zinc oxide nanowire-based artificial synapses with low-energy consumption. *J. Ind. Eng. Chem.*, **2020**, 88, 111–116.
- 36. Zhang, S.; Xu, W., All-printed ultra-flexible organic nanowire artificial synapses. *J. Mater. Chem*, **2020**, 8, 11138 11144.
- 37. Cui, Z.; Han, Y.; Huang, Q.; Dong, J.; Zhu, Y., Electrohydrodynamic Printing of Silver Nanowires for Flexible and Stretchable Electronics. *Nanoscale* **2018**, *10* (15), 6806-11.
- 38. Li, X.; Lee, G. S.; Park, S. H.; Kong, H.; An, T. K.; Kim, S. H., Direct Writing of Silver Nanowire Electrodes via Dragging Mode Electrohydrodynamic Jet Printing for Organic Thin Film Transistors. *Organic Electronics* **2018**, 62, 357-365.
- 39. He, B.; Yang, S.; Qin, Z.; Wen, B.; Zhang, C., The Roles of Wettability and Surface Tension in Droplet Formation During Inkjet Printing. *Sci. Rep.* **2017**, *7* (1), 11841.
- 40. Chaudhury, M. K.; Whitesides, G. M., Direct Measurement of Interfacial Interactions between Semispherical Lenses and Flat Sheets of Poly(Dimethylsiloxane) and Their Chemical Derivatives. *Langmuir* **1991**, *7* (5), 1013-25.38. Bashir, M.; Bashir, S.; Khan, H. U.; John, W., Deposition of Polyacrylic Acid Films on PDMS Substrate in Dielectric Barrier Corona Discharge at Atmospheric Pressure. *Surf. Interface Anal.* **2018**, *50* (9), 879-88.
- 41. Kim, H. T.; Jeong, O. C., PDMS surface modification using atmospheric pressure plasma. *Microelectron. Eng.* **2011**, *88* (8), 2281-5.
- 42. Xu, F.; Lu, W.; Zhu, Y., Controlled 3D Buckling of Silicon Nanowires for Stretchable Electronics. *ACS Nano* **2011**, *5* (1), 672-8.

- 43. Efimenko, K.; Wallace, W. E.; Genzer, J., Surface Modification of Sylgard-184 Poly(Dimethyl Siloxane) Networks by Ultraviolet and Ultraviolet/Ozone Treatment. *J. Colloid Interface Sci.* **2002**, *254* (2), 306-15.
- 44. Oláh, A.; Hillborg, H.; Vancso, G. J., Hydrophobic Recovery of UV/Ozone Treated Poly(Dimethylsiloxane): Adhesion Studies by Contact Mechanics and Mechanism of Surface Modification. *Appl. Surf. Sci.* **2005**, *239* (3-4), 410-23.
- 45. Chien, H. W.; Kuo, W. H.; Wang, M. J.; Tsai, S. W.; Tsai, W. B., Tunable Micropatterned Substrates Based on Poly(Dopamine) Deposition via Microcontact Printing. *Langmuir* **2012**, *28* (13), 5775-82.
- 46. Korte, K. E.; Skrabalak, S. E.; Xia, Y. N., Rapid Synthesis of Silver Nanowires through a CuCl- or CuCl₂-Mediated Polyol Process. *J. Mater. Chem.* **2008**, *18* (4), 437-41.
- 47. Hatipogullari, M.; Wylock, C.; Pradas, M.; Kalliadasis, S.; Colinet, P., Contact Angle Hysteresis In a Microchannel: Statics. *Phys. Rev. Fluids* **2019**, *4* (4), 1-21.
- 48. Drelich, J. W., Contact Angles: From Past Mistakes to New Developments Through Liquid-Solid Adhesion Measurements. *Adv Colloid Interface Sci* **2019**, *267* (267), 1-14.
- 49. Ding, Y.; Weng, L. T.; Yang, M.; Yang, Z.; Lu, X.; Huang, N.; Leng, Y., Insights into The Aggregation/Deposition and Structure of a Polydopamine Film. *Langmuir* **2014**, *30* (41), 12258-69.
- 50. Hong, S.; Na, Y. S.; Choi, S.; Song, I. T.; Kim, W. Y.; Lee, H., Non-Covalent Self-Assembly and Covalent Polymerization Co-Contribute to Polydopamine Formation. *Adv. Funct. Mater.* **2012**, *22* (22), 4711-4717.
- 51. Lee, H.; Dellatore, S. M.; Miller, W. M.; Messersmith, P. B., Mussel-Inspired Surface Chemistry for Multifunctional Coatings. *Science* **2007**, *318* (5849), 426-30.

- 52. Hillborg, H.; Tomczak, N.; Olah, A.; Schonherr, H.; Vancso, G. J., Nanoscale Hydrophobic Recovery: A Chemical Force Microscopy Study of UV/Ozone-Treated Cross-Linked Poly(Dimethylsiloxane). *Langmuir* **2004**, *20* (3), 785-94.
- 53. Fan, J. A.; Yeo, W. H.; Su, Y.; Hattori, Y.; Lee, W.; Jung, S. Y.; Zhang, Y.; Liu, Z.; Cheng, H.; Falgout, L.; Bajema, M.; Coleman, T.; Gregoire, D.; Larsen, R. J.; Huang, Y.; Rogers, J. A., Fractal Design Concepts for Stretchable Electronics. *Nat. Commun* **2014**, *5*, 3266.

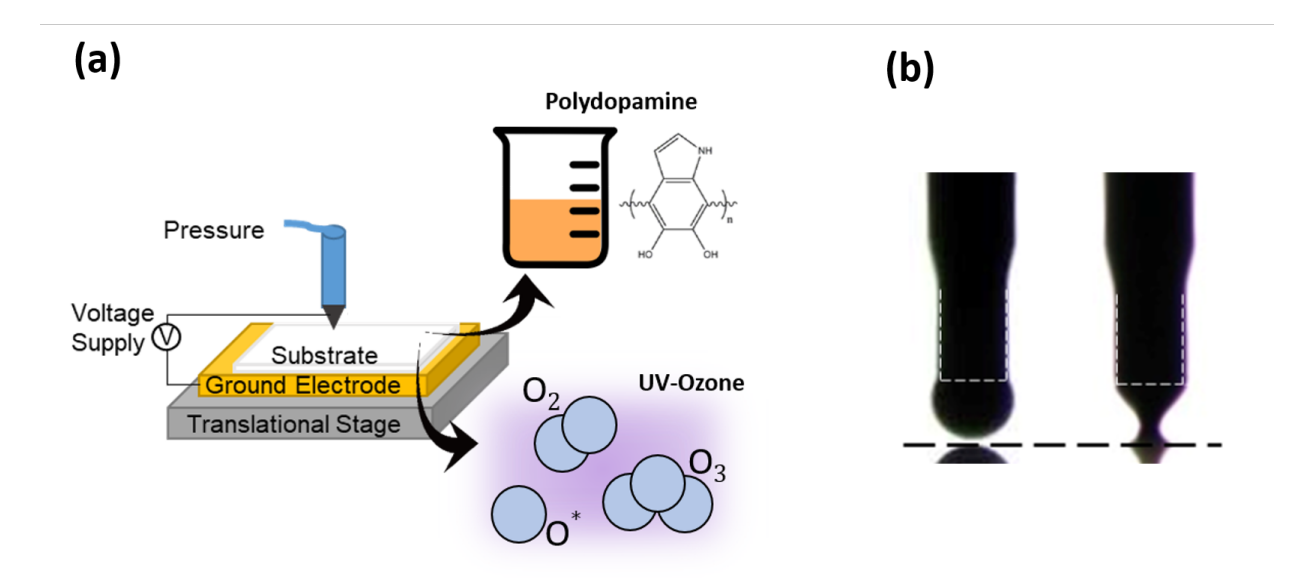


Figure 1. a) Schematic of the two surface treatment methods and EHD printing; b) Ink at the nozzle tip only with pressure (left), and Taylor cone and a stable jet formed with applied voltage (right).

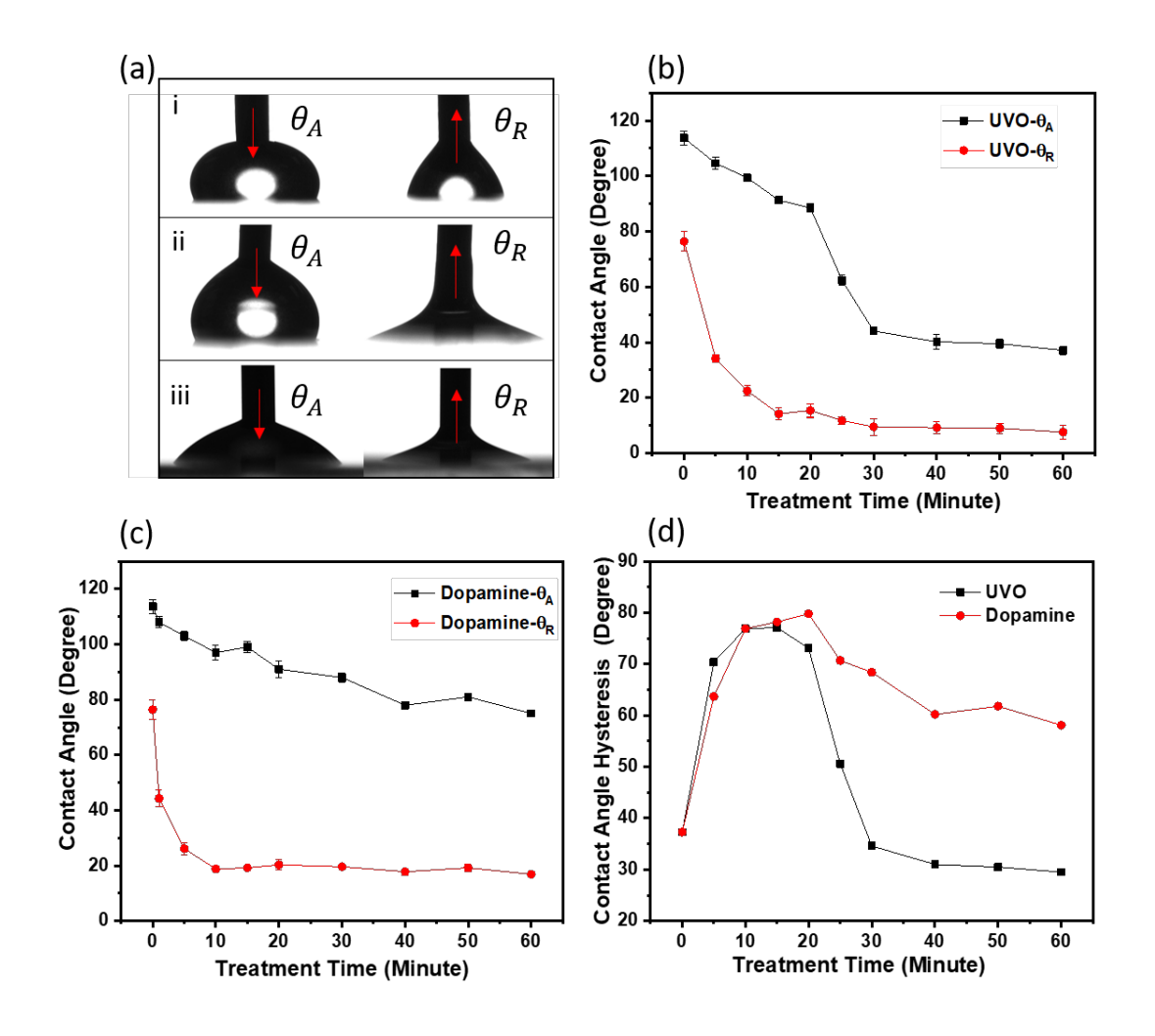


Figure 2. a) Optical images of advancing contact angle (θ_A) and receding contact angle (θ_R) of (i) untreated PDMS, (ii) PDMS treated with dopamine and (iii) PDMS treated with UVO; b) θ_A and θ_R vs. treatment time for PDMS modified with UVO treatment; c) θ_A and θ_R vs. treatment time for PDMS modified with dopamine. d) CAH vs. treatment time for PDMS modified with UVO and dopamine. Results presented were averaged from five experiments and expressed as the mean \pm SD.

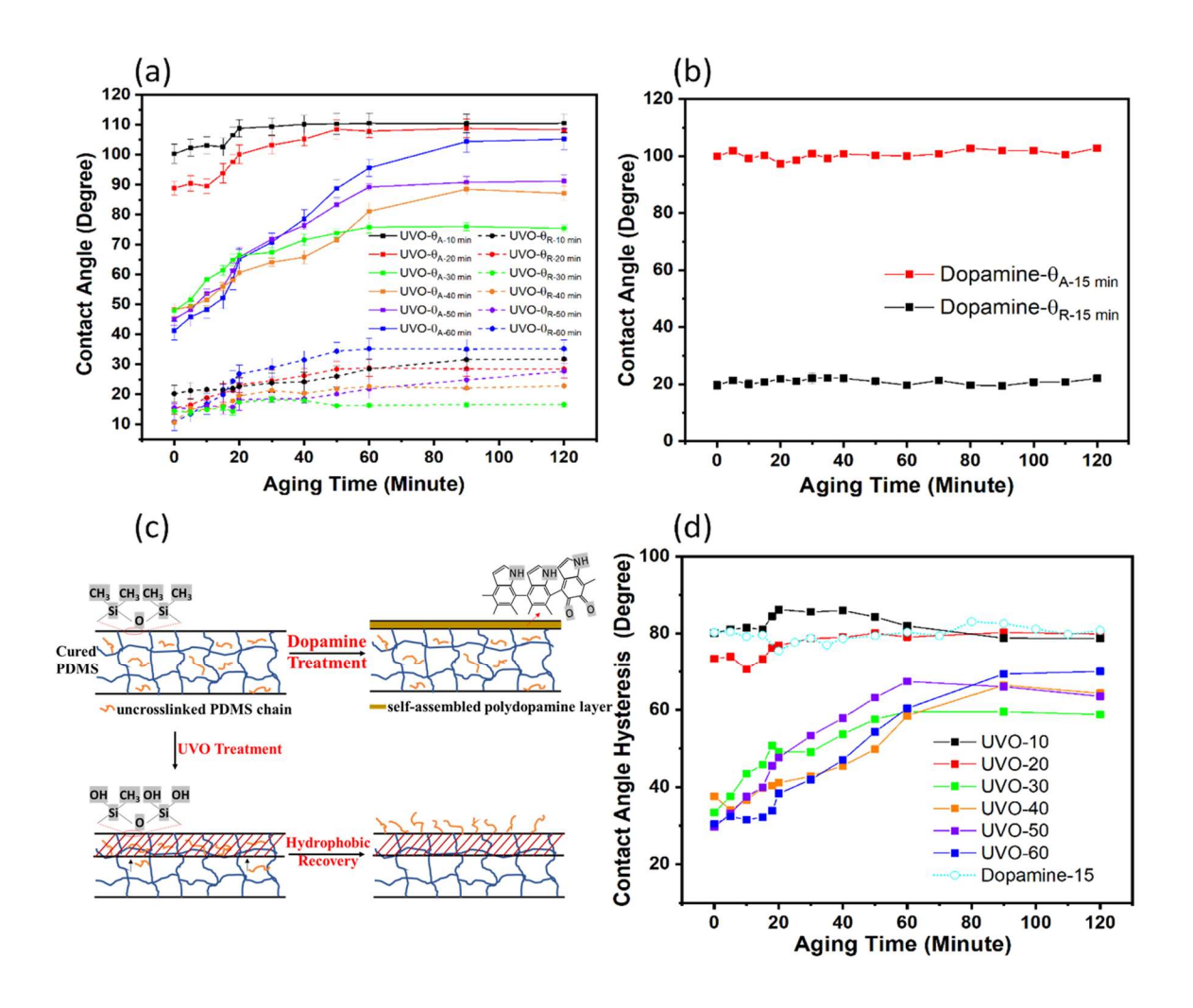


Figure 3. a) Contact angles vs. aging time for PDMS modified with UVO treatment (10, 20, 30, 40, 50 and 60 min). b) Contact angle vs. aging time for PDMS modified with 15 min dopamine pre-coating. c) Schematic of surface modification mechanism and aging effect of UVO treated PDMS and dopamine treated PDMS. d) CAH vs. aging time for PDMS modified with UVO treatment (10, 20, 30, 40, 50 and 60 min) and dopamine treatment (15 min). Results presented were averaged from five experiments and expressed as the mean ± SD.

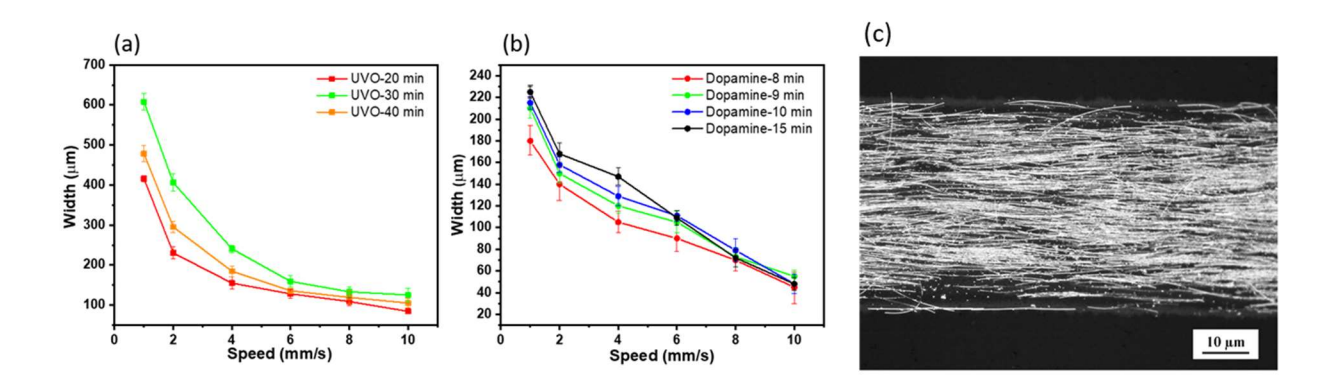


Figure 4. a) The linewidth measured at different printing speed when PDMS were treated with UVO treatment for 20 min, 30 min and 40 min; b) The linewidth measured at different printing speed when PDMS were treated with dopamine for 8 min, 9min, 10min and 15 min. Results presented were averaged from 20 positions on 5 lines and expressed as the mean \pm SD; c) The optical microscopy image of the printed conductive lines with the resolution of ~50 μ m.

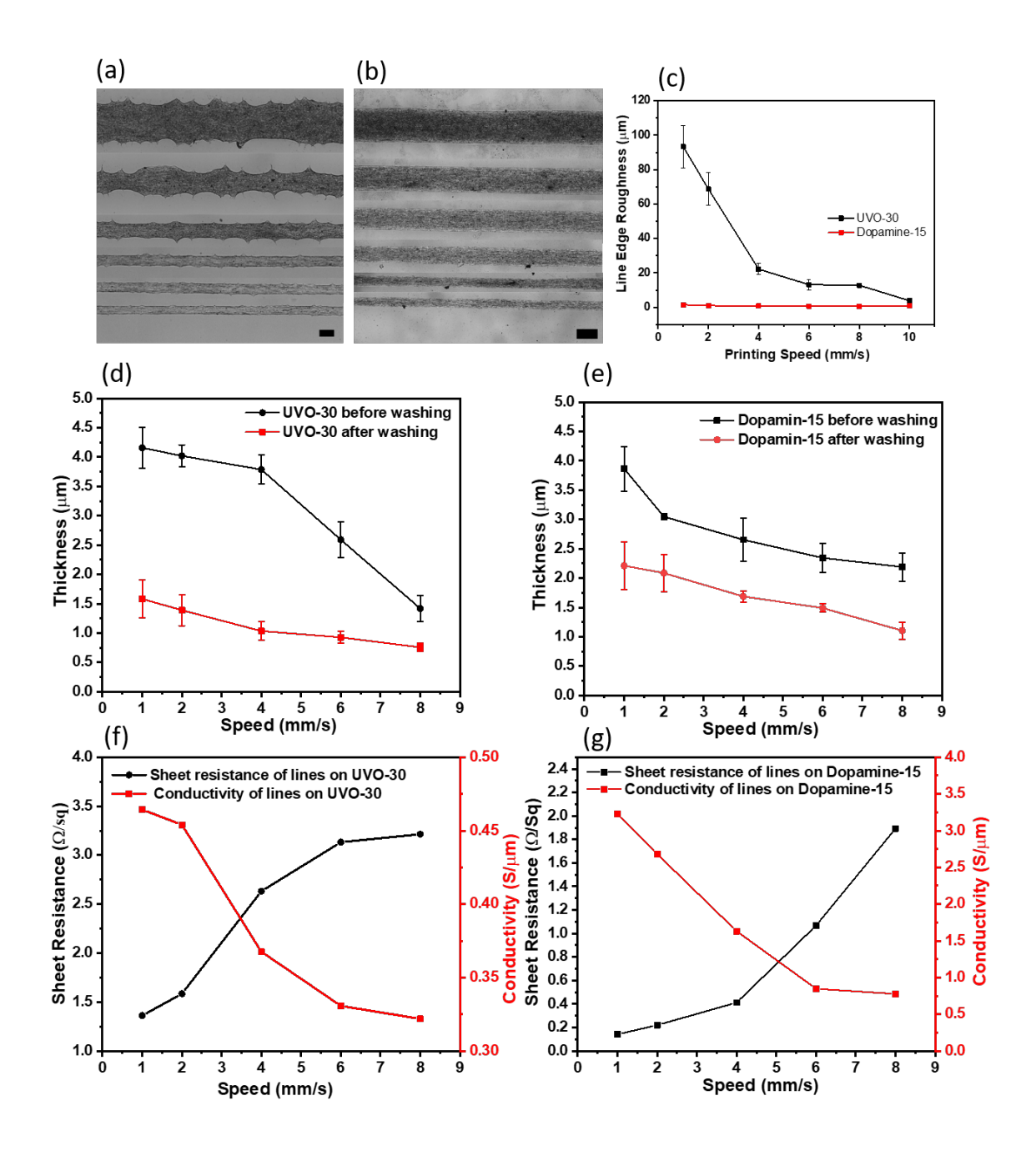


Figure 5. Optical images of printed lines at different printing speed on a) UVO-30 and b) Dopamine-15. Scale bars 200 µm. The printing speeds were 1, 2, 4, 6, 8 and 10 mm/s (from top to bottom) in both cases. c) The line edge roughness of the lines vs. the printing speed for UVO-30 and Dopamine-15. The line thickness vs. the printing speed before and after washing by water for d) UVO-30 and e) Dopamine-15. The sheet resistance and conductivity of the printed lines vs. the printing speed for f) UVO-30 and g) Dopamine-15. Edge roughness and thickness results presented were averaged from 4 different scanned location along printed lines and expressed as the mean ± SD.

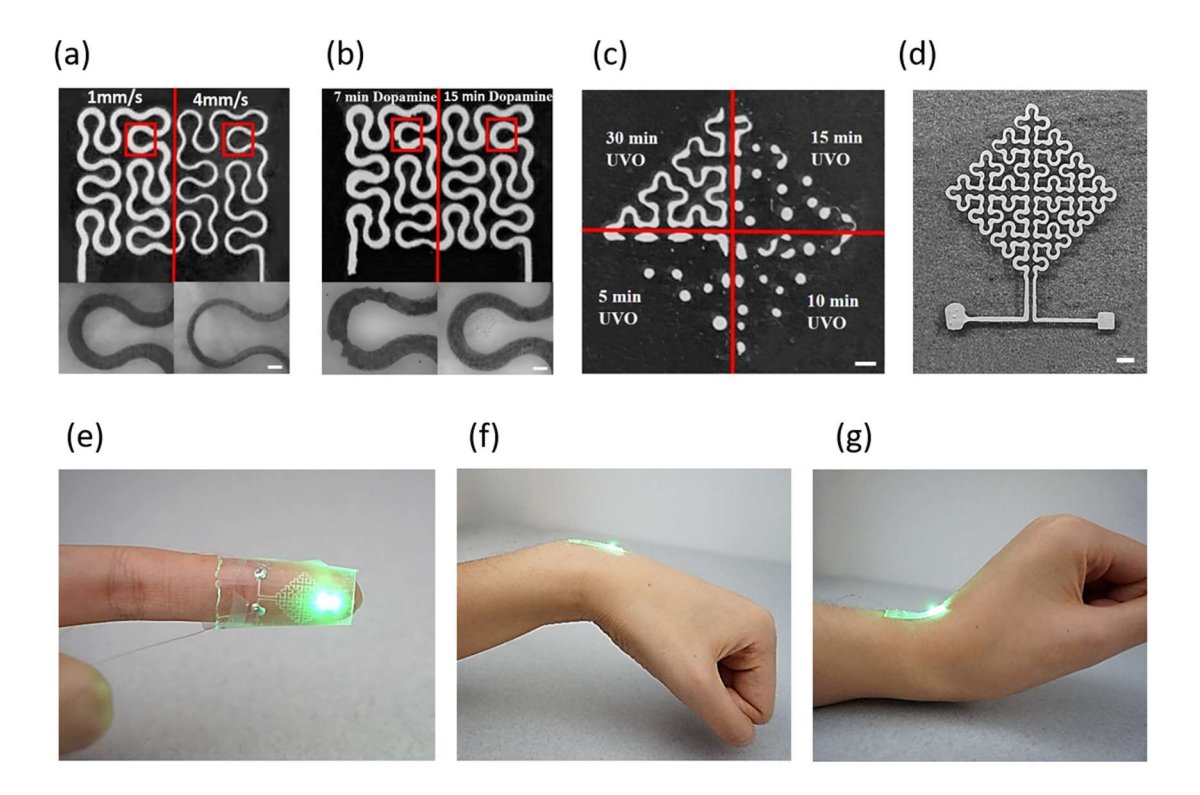


Figure 6. Peano curve printed on a) dopamine treated PDMS at printing speeds of 1 and 4 mm·s⁻¹ and. Scale bars 200 μm. b) Peano curve printed on a dopamine treated PDMS with two regions that were treated by 7 and 15 min each. Scale bar 200 μm. c) Sierpinski curve printed on a UVO treated PDMS with four regions that were treated by 5, 10, 15 and 30 min each. Scale bar 1 mm. d) Sierpinski curve printed on PDMS treated with dopamine for 15 min. Scale bar 1 mm. e) Printed thin patch electronics rounded a fingertip. The printed thin patch electronics remained stable while wrist was bent f) forward and g) backward.

Table of Contents

